Electron energy loss spectroscopy of acetone vapor*

Russell H. Huebner
Argonne National Laboratory, Argonne, Illinois 60439

R. J. Celotta, S. R. Mielczarek, and C. E. Kuyatt
National Bureau of Standards, Washington, D.C. 20234

(Received 12 June 1973)

High resolution, inelastic electron scattering data can provide new spectroscopic information on the electronic structure of polyatomic molecules. Features in the acetone energy loss spectrum from 0 to 15 eV obtained for 100 eV incident electrons correspond to vibrational, electronic discrete, and electronic continuum excitations. These data are compared with optical measurements in a wide spectral region extending from the infrared to the vacuum ultraviolet. A comprehensive interpretation of the energy loss spectra is attempted with the use of photochemical and photoelectron data, as well as quantum-chemical calculations in the literature. Three Rydberg series with quantum defects of 1.03, 0.81, and 0.315 join onto bands previously discussed in terms of transitions to valence orbitals. These series converge to an ionization limit of 9.705 eV in good agreement with previous optical determinations. Dissociative continua underlie the Rydberg region and give rise to a variety of neutral products observed in recent photolysis work. Broad features in the ionization continuum appear to correlate generally with higher ionization potentials observed by photoelectron spectroscopy. Apparent oscillator strengths derived from the energy loss data for the bands at 4.4 and 6.35 eV and for a region (9.7–11.78 eV) of the ionization continuum agree very well with the photoabsorption measurements. Integrated oscillator strengths of 0.46 below 9.7 eV and 3.93 below 15 eV were derived from the electron impact data.

I. INTRODUCTION

A recent electron energy loss study of formaldehyde[1] has prompted a similar study of a structurally related molecule, acetone, where methyl groups replace the hydrogen atoms bound to the carbonyl group, $\geq C=O$. Molecules containing the carbonyl group are common bases for the formation of a hydrogen bond with other proton donor molecules.[2] Consequently, they are frequently implicated in many chemical and biological mechanisms such as solvent shifts in optical absorption spectra and protein linkage.

Previous spectroscopic studies[3–8] of the photoabsorption spectrum of acetone vapor show regions of both continuous and discrete transitions and have recently been extended[9] above the ionization potential (I. P.) at 9.7 eV. However, only the lowest absorption band has been definitely assigned to the $n \rightarrow \pi^*$ transition through valence orbital calculations. Moreover, at least one[10] and possibly a second[11] Rydberg series observed by photoabsorption have not yet been taken into account in any quantitative theoretical analysis of the acetone spectrum.

Only three electron impact studies of the acetone spectrum have previously been reported. Electron energy loss spectra of acetone were first obtained by Silverman and Lassettre[12] for incident kinetic energies of 220 and 500 eV. Although these spectra were obtained at comparatively low resolution, they were in quantitative agreement with optical spectra. Threshold electron impact studies[13,14] of acetone have indicated a negative ion resonance at about 1.6 eV, and also the lowest triplet state at about 4.15 eV. However, the low resolution achieved in these studies (~ 0.2 eV) renders interpretation of excitation processes observed at higher energies rather tenuous.

In the present study, high resolution electron energy loss spectra of acetone were obtained for 100 eV incident electrons scattered at zero angle. The data are discussed with reference to other spectroscopic information which includes recent photoelectron[15] and pressure broadening[16] studies. An apparent oscillator strength distribution is derived from the energy loss spectrum and compared with optically determined values.

II. EXPERIMENTAL

The instrument used to obtain the spectrum of acetone is described in detail elsewhere.[17–19] Briefly, the NBS Model AN-1 electron-spectrometer system consists of two major sections—a monochromator and an analyzer. The monochromator generates a collimated electron beam, defines a narrow energy spread about the mean energy of the incident beam, and focuses it into a collision chamber. From the monochromator, the electrons enter the collision chamber which is differentially pumped. In usual operation, sample gas pressures from a few millitorr to 0.1 torr are maintained in the collision region with the rest of the electron–optical system held at approxi-

mately 10^{-6} torr.

Electrons leaving the collision chamber pass through an acceleration region and into the analyzer section. Initially the analyzer section is adjusted to allow only electrons that have not lost energy to reach the detector. All electrons that have lost energy are deflected away by the electrostatic hemispheres. Later, a precisely known accelerating voltage is applied at the entrance to the analyzer section so that only electrons with energy losses equal to the applied potential can then reach the detector. These electrons are counted with an electron-multiplier detector. The number of electrons analyzed in each 10 meV interval was counted and stored in an on-line computer operated in a multichannel scaling mode.

The spectrum was swept between two selected energy loss points, alternately for increasing and decreasing energy loss, for 50 sweeps with the count accumulated in each channel. The counting time per channel in each sweep was 17 msec.

In the present study, only electrons scattered in the forward direction within an approximate maximum acceptance angle of 0.02 rad were observed. Although the maximum acceptance angle $\hat{\theta}$ is not well defined in this system, the estimate of $\hat{\theta} = 0.02$ rad was made from a computer analysis of limiting electron trajectories through the analyzer for typical operating conditions.

Approximately equal parts of helium (0.1091 torr) and acetone (0.1671 torr), where the pressures were measured with a capacitance manometer, were leaked together into the apparatus. The $2^1P \leftarrow 1^1S$ transition in helium at 21.21 eV was then used as a calibration point of the energy loss scale, and the full width at half-maximum (FWHM) of this transition peak was determined as an experimental check on the energy resolution of the system. Since all of the electronic transitions from the helium ground state occur at energies greater than 19.8 eV, they do not contribute to the spectrum at lower energies. The spectra presented in this paper were obtained with an incident electron beam of mean energy T equal to 100 eV and a total system resolution of 36 meV FWHM.

III. SPECTROSCOPIC ANALYSIS

A. Vibrational Excitation

The spectrum of acetone vapor for energy losses from 0 to 10 eV is shown in Fig. 1. The high intensity observed at 0 eV is due to electrons that have passed through the collision chamber without energy loss. Superimposed on the rapidly declining tail of the unscattered beam are several peaks. These correspond to vibrational excitations of the acetone molecule in its ground electronic state. This region is shown on an expanded scale in the insert in Fig. 1. Analysis of the energy losses observed in this region show qualitative agreement with observed infrared absorption energies.[20,21] The broad peak centered at about 0.16 eV is a composite of several unresolved vibrational excitations, principally the (ν_{17}) C–C stretch

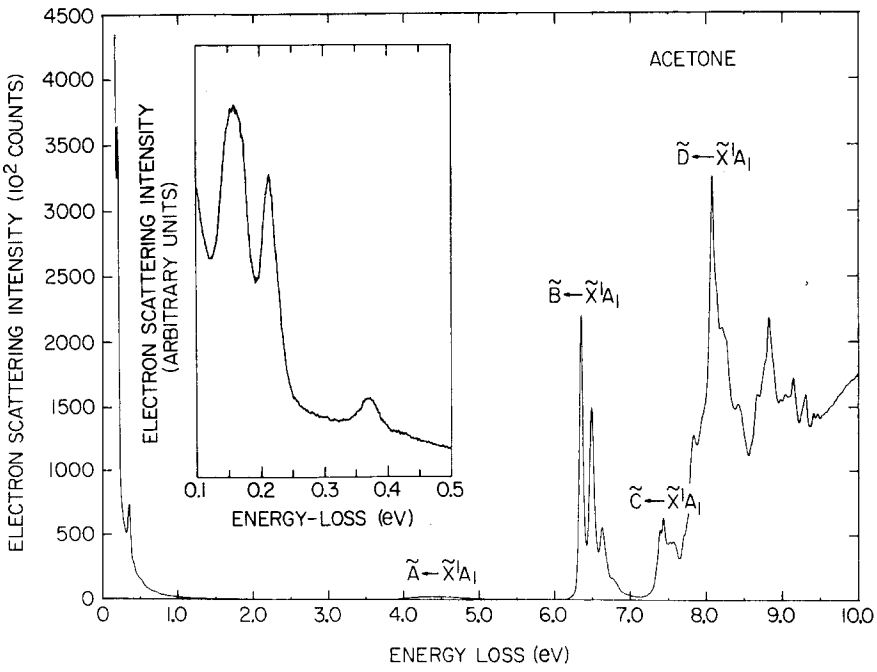

FIG. 1. Energy loss spectrum of acetone vapor from 0 to 10 eV for 100 eV incident electrons scattered within 0.02 rad of the incident direction. The insert shows the vibrational excitation region on an expanded energy scale for an instrumental resolution of 22 meV.

TABLE I. Excitation of vibrational modes by electron impact.

Energy loss peak energy (eV)	Energy (eV)	Ground state vibrational modes[a] Approximate type	No.	Sym. class
0.160	0.151	C–C stretch	ν_{17}	b_1
	0.169	CH_3 sym. deform.	ν_5, ν_{16}	a_1, b_1
	~0.175	CH_3 deg. deform.	$\nu_4, \nu_{15}, \nu_{21}$	a_1, b_1, b_2
0.215	0.215	C–O stretch	ν_3	a_1
0.370	0.365	CH_3 sym. stretch	ν_2, ν_{14}	a_1, b_1
	0.368	CH_3 deg. stretch	ν_{20}	b_2
	0.374	CH_3 deg. stretch	ν_1, ν_{13}	a_1, b_1

[a]Taken from Refs. 20 and 21.

mode (0.151 eV) and the (ν_5, ν_{16}) CH_3 symmetric deformation modes (0.169 eV) and to a lesser extent, the (ν_4, ν_{15}, ν_{21}) CH_3 degenerate deformation modes (0.175 to 0.178 eV). The sharp peak observed at 0.215 eV arises from excitation of the (ν_3) C–O stretch mode (0.215 eV) alone. At about 0.37 eV a broad but weaker band appears due to several (ν_1, ν_{13}, ν_2, ν_{14}, ν_{20}) CH_3 symmetric and degenerate stretch modes (0.365 to 0.374 eV). Excitation of vibrational modes corresponding to energy losses below about 0.15 eV were obscured by the zero loss beam. Evidence for the excitation of two vibrational quanta of one mode or a combination of two modes is indicated in the energy loss region around 0.42 eV, corresponding to two quanta of the C–O stretch (ν_3) mode. These are summarized in Table I.

B. Electronic Excitation

Although there have been several experimental[3–8] and interpretive[22–25] studies of transitions to the excited states of acetone, there nevertheless remains considerable uncertainty regarding the assignment of specific transitions for the spectral features observed. This circumstance is due largely to the absence of a unifying theoretical treatment that includes both Rydberg and valence configurations in the calculation of transition energies and probabilities for this molecule. Although such extensive calculations have recently been reported for formaldehyde,[26,27] they have not been extended to acetone. Thus, the empirical labels utilized by Herzberg[28] will be adopted in the following discussion.

Four energy loss bands are observed in the regions near 4.5, 6.5, 7.5, and 8.1 eV in Fig. 1. The excited states are designated with empirical labels $\tilde{A}$, $\tilde{B}$, $\tilde{C}$, and $\tilde{D}$, with the ground state denoted by $\tilde{X}\ ^1A_1$.

1. The $\tilde{A} \leftarrow \tilde{X}\ ^1A_1$ Transition Region

The structureless band ($\tilde{A} \leftarrow \tilde{X}\ ^1A_1$) with a maximum at 4.42 eV has been observed by several workers,[3,6,12] who assign it to a singlet $n_O \rightarrow \pi^*$ transition. Allinger *et al.*[24] calculate that such a transition should occur at 4.39 eV. Since this transition is forbidden, the band is expected to be very weak. The smoothness of the band is indicative of a dissociative continuum, although some discrete structure, particularly at the low-energy side, has been reported (see Herzberg[28] for further discussion). This structure was not apparent in the energy loss spectrum.

Photolysis experiments carried out in this region[29–32] indicate that the dominant dissociative process is

$$(CH_3)_2\,CO + h\nu \rightarrow (CH_3)_2\,CO^* \rightarrow CH_3CO \text{ and } CH_3. \quad (1)$$

Potapov and Shigorin[33] postulate that one electron excited from a nonbonding oxygen orbital (n_O) to the antibonding π orbital (π^*) of the carbonyl bond leaves a nonbonding orbital on the oxygen unfilled. A σ electron from a C–C bond then associates with the remaining electron in the n_O orbital through an exchange interaction. This association leads to a rupture of a C–C bond and formation of a triple bond between carbon and oxygen atoms with the resulting dissociation into methyl and acetyl radicals. However, several studies[30,32,34] have suggested that dissociation occurs from a triplet state after intersystem crossing. The latter explanation is preferred in the theoretical treatment[35] of dissociation of formaldehyde in the $n_O \rightarrow \pi^*$ absorption region.

2. The $\tilde{B} \leftarrow \tilde{X}\ ^1A_1$ Transition Region

The $\tilde{B} \leftarrow \tilde{X}\ ^1A_1$ transition comprises three distinct peaks in the energy loss spectrum (Fig. 1) located at 6.35, 6.49, and 6.63 eV and a shoulder

at about 6.77 eV. The regular spacing of 140±10 meV between these peaks is indicative of vibrational fine structure and corresponds closely to the frequency difference of 1194 cm^{-1} (148 meV) observed optically.[5,7,11] By comparison with the related band structure of deuteroacetone, Lawson and Duncan[5] concluded that this vibration corresponds to bending of the HCH bond angles in the methyl groups (i.e. CH_3 symmetric deformation modes ν_5 and ν_{16} in Table I).

McMurry[22] assigned the $\tilde{B} \leftarrow \tilde{X}\ ^1A_1$ band to a transition from the nonbonding orbital to an antibonding σ orbital ($n_O \rightarrow \sigma^*$) with the reservation that a Rydberg transition could contribute part or even all of the energy absorption observed in this region. Although several workers[8,25] differed with this assignment, it appeared generally accepted that for acetone[6,12] and other carbonyls[23,36-38] the second band arose from an allowed $n_O \rightarrow \sigma^*$ transition. Two recent experiments, however, emphasize the Rydberg character of this band. In a study of the $\tilde{B} \leftarrow \tilde{X}\ ^1A_1$ absorption band in acetone as the pressure of a perturber gas (N_2) was increased, Robin and Kuebler[16] observed considerable broadening characteristic of a Rydberg upper state. However, since the pressure effect was not extreme, they concluded that the upper ($\tilde{B}$) state must be of mixed Rydberg–valence orbital character. Also, in the photoelectron spectrum of acetone recently reported by Brundle *et al.*[15] the first band, corresponding to the ejection of an electron from the nonbonding orbital, shows a nearly identical profile and vibrational spacing as that observed for the $\tilde{B} \leftarrow \tilde{X}\ ^1A_1$ band. This also indicates that energy absorption in the $\tilde{B}$ region is associated with a $n_O \rightarrow$ Rydberg transition.

The broadness of the peaks in this band are particularly noticeable for the peak at 6.63 eV and the diffuse shoulder at 6.77 eV and does not appear to be entirely instrumental. It is likely that some broadening due to predissociation occurs in this region. Although no exhaustive study of photodissociation in this region has been carried out, the photolysis work of Potzinger and von Bünau[39] at the single wavelength 185 nm (6.7 eV) indicates a quantum yield of 1.0 for the production of CO independent of temperature, pressure, and the presence of scavengers. They propose the simple mechanism

$$(CH_3)_2\,CO + h\nu \rightarrow (CH_3)_2\,CO^* \rightarrow 2CH_3 + CO, \qquad (2)$$

which accounts for more than 90% of all subsequent products observed.

3. *The $\tilde{C} \leftarrow \tilde{X}\ ^1A_1$ and $\tilde{D} \leftarrow \tilde{X}\ ^1A_1$ Transition Regions*

The region between 7.2 and 8.0 eV and the region near 8.1 eV correspond to the transition regions labeled by Herzberg[28] as $\tilde{C} \leftarrow \tilde{X}\ ^1A_1$ and $\tilde{D} \leftarrow \tilde{X}\ ^1A_1$, respectively. Four peaks in the energy loss spectrum at 7.39, 7.44, 7.52, and 7.56 eV are evident and an additional shoulder at about 7.71 eV and a peak at 7.84 eV also appear in the $\tilde{C}$ region. Assignment of features observed in this region on the basis of previous optical work has been extremely tenuous. Barnes and Simpson[8] suggested assignment as a $n_O \rightarrow \sigma^*$ transition, although the observed intensity is much lower than theoretical prediction.[22] Allinger *et al.*[24] predicted a transition from a bonding π orbital ($\pi \rightarrow \pi^*$) should occur at an energy of 7.41 eV, but again with much more intensity. They concluded in agreement with McMurry[22] that the $\pi \rightarrow \pi^*$ transition must actually lie at higher energies. The proximity of this region to the Rydberg region (discussed further in the following section) adds still other possible alternative interpretations for the structure in the $\tilde{C}$ region. No photochemical studies have been carried out at these energies.

The most intense discrete feature in the acetone energy loss spectrum occurs at 8.08 eV with additional shoulders and peaks at higher energies. Watanabe[10] first identified this transition ($\tilde{D} \leftarrow \tilde{X}\ ^1A_1$) as a member of a Rydberg series converging to an I.P. = 9.705 eV. The assignment of this Rydberg series and others will be discussed in the following section.

The diffuse absorption[4] underlying the $\tilde{D}$ region may be taken as evidence for transitions to possible valence or mixed Rydberg–valence states leading to dissociation. Photolysis experiments[40,41] with the 147 nm (8.43 eV) xenon resonance line indicate at least four important primary dissociation mechanisms:

$$(CH_3)_2\,CO + h\nu \rightarrow \begin{cases} CH_3COCH_2^* + H \\ \quad\rightarrow CH_2CO + CH_3, \end{cases} \qquad (3)$$

$$(CH_3)_2\,CO + h\nu \rightarrow \begin{cases} CH_3COCH^* + H_2 \\ \quad\rightarrow C_2H_4 + CO, \end{cases} \qquad (4)$$

$$(CH_3)_2\,CO + h\nu \rightarrow (CH_3)_2CO^* \rightarrow CH_2CO + CH_4, \qquad (5)$$

and

$$(CH_3)_2\,CO + h\nu \rightarrow (CH_3)_2CO^* \rightarrow CO + 2\,CH_3\,. \qquad (6)$$

Quantum yields for these dissociation products have been recently measured by Lin and Ausloos.[41] Potapov and Shigorin[33] have argued that dissociation of a hydrogen atom should occur in the region near 7.9 eV following excitation of the $\pi \rightarrow \pi^*$ transition in accord with the mechanism (3). Mechanism (6) is identical to the dissociation mechanism (2) found for the $\tilde{B}$ band and may also be associated with a Rydberg transition. The remaining mechanisms leading to the production of

TABLE II. Rydberg series for acetone.

n	Series I peak energies (eV)				Series II peak energies (eV)		Series III peak energies (eV)		
	(a)	(b)	(c)	(d)	(c)	(d)	(b)	(c)	(d)
3			6.35	6.20	7.39 (7.44)	6.92	7.84	7.84 (7.71)	7.82
4	8.08	8.09	8.08	8.16	8.42	8.42	8.70	8.68	8.70
5	8.84	8.84	8.83	8.84	8.98	8.98	9.08	9.04	9.08
6	9.15	9.16	9.15	9.15	(9.25)	9.25	9.28	9.28	9.28
7	9.34	9.33	9.31	9.32		9.40	(9.41)	(9.41)	9.40
8	9.43	9.42	9.42	9.42		9.49			9.47
9	9.49	9.48	9.47	9.49		9.55			9.52
10		9.54	9.54	9.54		9.59			9.56

[a]Optical data of Watanabe (Ref. 10).
[b]Optical data of Lyu (Ref. 11).
[c]Electron energy loss data (present work).
[d]Calculated Rydberg peak positions with values for series I: IP = 9.705 eV, $\delta = 1.03$; series II: IP = 9.755 eV, $\delta = 0.81$; and series III: IP = 9.705 eV, $\delta = 0.315$.

molecular hydrogen and methane have not been related to specific electronic transitions.

4. *The Rydberg Transition Region*

For the purposes of discussion of present results, we have chosen to define the Rydberg region as extending from 6.0 eV to the ionization potential of acetone, although Rydberg transitions associated with higher ionization limits can occur at higher energies. This region, which overlaps the $\tilde{B}$, $\tilde{C}$, and $\tilde{D}$ regions, is shown on an expanded energy loss scale in Fig. 2.

Watanabe[10] identified a strong Rydberg series starting at about 8 eV and converging to an I. P. = 9.705 eV. Most of the peak energies E_n were fitted by the Rydberg formula

$$E_n = \text{I. P.} - R/(n-\delta)^2 , \tag{7}$$

where $R = 13.606$ eV, $\delta = -0.97$, and $n = 2, 3, 4 \cdots$. More recently, this series has been discussed by Herzberg[28] and Duncan[42] for an equivalent choice of $\delta = 0.03$ with $n = 3, 4, 5 \cdots$. This series identification was confirmed in the unpublished work of Lyu,[11] and in addition, he identified a second, weaker series converging to an I. P. = 9.689 eV with $\delta = -0.68$ and $n = 2, 3 \cdots$. From the present electron energy loss data we identify three Rydberg series in acetone which are compared in Table II with the photoabsorption data.

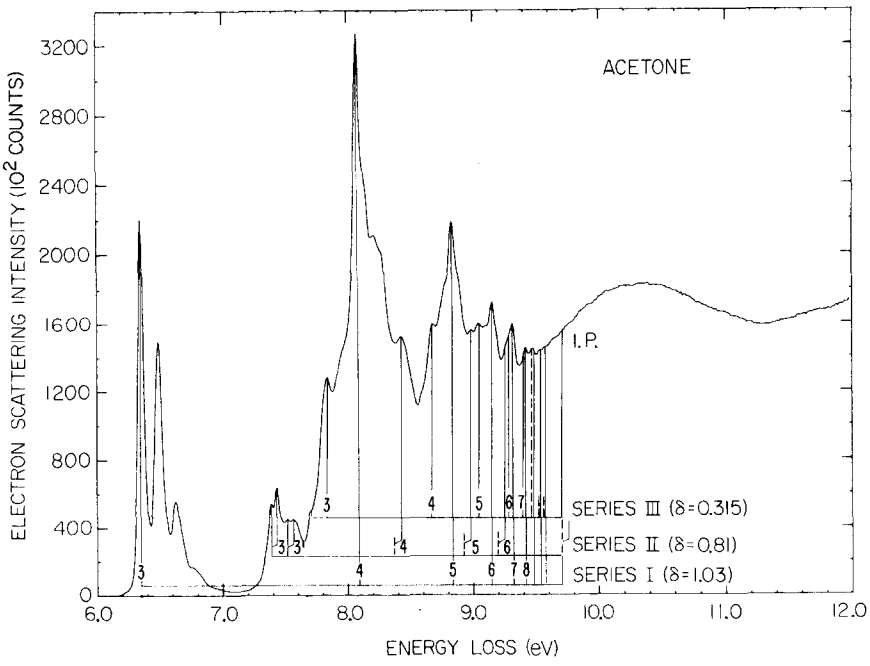

FIG. 2. Energy loss region from 6 to 12 eV detailing the three Rydberg series identified for acetone.

The principal members of each series are indicated by vertical lines connected by a horizontal bar. The numbers indicated for each member are our revised assignments of the principal quantum numbers for the values of I. P. and δ (given in Table II) determined from the electron impact data.

The strong Rydberg series (Series I) includes the most intense peak at 8.09 eV previously identified as $\tilde{D} \leftarrow \tilde{X}\ ^1A_1$. By choosing $\delta = 1.03$ rather than $\delta = 0.03$ and advancing n by unity, we obtain the same series as first identified by Watanabe[10] converging to I. P. = 9.705 eV. However, this choice then places the $n = 3$ member at 6.20 eV, close to the $\tilde{B} \leftarrow \tilde{X}\ ^1A_1$ band. From the earlier discussion then it is consistent to associate the Rydberg character of the $\tilde{B} \leftarrow \tilde{X}\ ^1A_1$ band with series I. The $n = 4$ Rydberg member is superimposed on a region of continuous absorption which accounts for the large intensity increase from the $n = 3$ member. The $\pi \rightarrow \pi^*$ dissociative continuum, as suggested by the photolysis work,[41] possibly contributes to the underlying intensity near 8.1 eV.

The large quantum defect, $\delta = 1.03$, for series I points to assignment of series I as corresponding to the promotion of one electron from the nonbonding orbital to an "s" type Rydberg orbital (i.e. $n_O \rightarrow ns$). This follows the assignment of a similar series in formaldehyde with $\delta = 1.04$, and has been suggested for acetone previously by LaPaglia[43] and Duncan.[42]

Lyu[11] first observed series III by photoabsorption and yet there does not appear to be any published discussion of the occurrence of this series. The observed peak positions for this series (see Table II) are fitted by the Rydberg formula [Eq. (7)] for $\delta = 0.315$ and I. P. = 9.705 eV. Our value for I. P. is identical to that for series I and differs slightly from the value of 9.689 eV determined optically.[11] The quantum defect for this series is only slightly smaller than that for the "nd" series ($\delta = 0.4$) in formaldehyde, suggesting assignment of series III as $n_O \rightarrow nd$. Although we locate the $n = 3$ member of this series at the 7.84 eV peak, the shoulders at 7.71 and 7.96 eV may indicate splitting of the molecular symmetry components of the "$3d$" Rydberg orbital according to their different orientations in the molecular field. For Rydberg orbitals of higher n, these components rapidly become degenerate in energy.[43] Such a splitting has been discussed for the $3d$ Rydberg level in formaldehyde.[27]

Identification of series II from the energy loss data is based on the observation of three peaks and a shoulder which are not clearly accounted for by either series I or III. Members of this series for $n \geq 7$ are not evident, probably because they are weak and overlap with members of the stronger series I and III. Peak energies for this series were fitted by the Rydberg formula with $\delta = 0.81$ and I. P. = 9.755 eV. This ionization limit is 0.05 eV greater than that found for series I and III, which can be explained if the peaks correspond to excitation of one vibrational quantum (i.e., $h\nu = 0.05$ eV) in each respective Rydberg state rather than the O–O vibrational level. This interpretation is supported by the observation of a separation of 0.05 eV between the first two peaks of the $n = 3$ band at 7.39 and 7.44 eV, with the second peak having the greater intensity. Excitation of a vibrational quantum of similar magnitude, 0.045 eV, is also observed[15] in the photoelectron band for this ionization limit. The C–C–C deformation mode $\nu_8(a_1)$ with a quantum energy of 0.048 eV in the ground electronic state is a likely candidate for assignment here, although the C–O bending modes, $\nu_{19}(b_1)$ and $\nu_{23}(b_2)$ with ground state energies of 0.065 and 0.060 eV, are also possible.[20]

With a quantum defect of 0.81, this series corresponds most closely with the "np" Rydberg series in formaldehyde with $\delta = 0.7$.[42] Inclusion of the $\tilde{C} \leftarrow \tilde{X}\ ^1A_1$ band as the $n_O \rightarrow 3p$ member is in accord with the correlation suggested earlier by LaPaglia[43] and explains the difficulties discussed earlier in the assignment of this band by consideration of only valence orbital transitions. It is also expected[43] that the molecular symmetry components of the "$3p$" Rydberg orbital (i.e., $3pb_2$ and $3pa_1$ in formaldehyde) will split depending upon their respective orientations in the field of the molecular core. Thus the two peaks at 7.52 and 7.56 eV may be associated with the higher energy component of the split $3p$-Rydberg orbital. The energy difference of 0.13 eV between the peaks at 7.39 and 7.52 eV is reasonably close to the splitting of 0.16 eV observed for the $3pb_2$ and $3pa_1$ Rydberg orbitals of formaldehyde. Provided the identification and assignment of series II for acetone is correct, the weak intensities observed for this series in contrast to the strong $n_O \rightarrow np$ series in formaldehyde remain unexplained.

C. Continuum Excitation

Beyond 9.7 eV lies a broadly structured energy absorption continuum. Its principal features are broad maxima at 10.4, 12.3, 14.0, and 14.5 eV, as exhibited in Fig. 3. Silverman and Lassettre[12] reported similar features occurring at slightly lower energies. Structure in the continuum region results from both ionization and dissociation processes not fully investigated at present. Photoionization yield measurements[9,44] for acetone indicate that ionization accounts for about 25% of the energy absorption observed in the region near

10.4 eV. The ionization yield increases from this value above about 12.0 eV,[45] and an ionization quantum yield of unity is reported[46] at 16.8 eV.

Relative photoionization cross section measurements[47,48] indicate that both parent ion $(CH_3)_2CO^+$ and a fragment ion CH_3CO^+ are produced in the region below about 11.5 eV. The cross section for parent-ion production increases from the ionization threshold to about 10.45 eV. At this energy the fragment ion appears and increases almost linearly with increasing energy. The electron-impact ionization data of Dorman[49] and of Potapov and Shigorin[33] show similar ion fragmentation in this energy region. These data correlate with the broad maximum in the energy loss spectrum at about 10.4 eV and suggest the ejection of one of the nonbonding electrons from the molecule. At approximately 0.7 eV above the ionization threshold there is sufficient energy to induce dissociation of the parent ion into a fragment ion CH_3CO^+ and a methyl radical. Potapov and Shigorin[33] argue that the mechanism for dissociation of this ionic state is similar to that described previously for the $n_O \rightarrow \pi^*$ dissociation continuum at 4.4 eV. Also, at the same photon energies, the photolysis studies[41] indicate that dissociation mechanism (4) remains an important contributor to the production of molecular hydrogen and ethylene.

The broad maxima at 12.3, 14.0, and 14.5 eV in the energy loss spectrum correlate reasonably well with the higher ionization potentials at 12.6, 13.9, and 14.5 eV observed by photoelectron spectroscopy.[15] Additional ion fragments (e.g., CH_3^+, CH_4^+, HCO^+, CO^+, etc.) are reported[33,49] for electron impact energies above about 12.0 eV. However, further theoretical and experimental work is needed before definite assignments can be made.

IV. OSCILLATOR STRENGTHS

For sufficiently large incident electron energy T and small scattering angle $\theta \simeq 0$ the inelastic electron scattering intensity distribution $I(E)$ is related to the differential optical oscillator strength distribution df/dE. Such a relation will hold only over a limited range of energy losses, E, such that $E/T \ll 1$. For an apparatus with small circular apertures which define a finite maximum acceptance angle $\hat{\theta}$, the measured intensity will be proportional to the differential electron scattering cross section $d\sigma/d\Omega$ integrated over the finite solid angle $\Delta\Omega$, corresponding to $\hat{\theta}$. Thus,

$$I(E) \propto \Delta\sigma/\Delta\Omega = \int \frac{d\sigma}{d\Omega} d\Omega \Big/ \int d\Omega \tag{8}$$

where $d\Omega = 2\pi \sin\theta \, d\theta$. Using the Born approximation expression[50] for $d\sigma/d\Omega$ and further assuming that the generalized oscillator strength $df(K)/dE$ can be approximated by the optical oscillator strength for small values of momentum transfer K, one can derive the expression

$$df/dE \propto (E/R)\,\hat{\theta}\,\{\ln[1+(\hat{\theta}/\gamma)^2]\}^{-1}\, I(E)\,, \tag{9}$$

where

$$\gamma^2 = (E/2T)^2\,(1-E/T)^{-1} \quad \text{for constant } T.$$

However, this expression neglects the second and

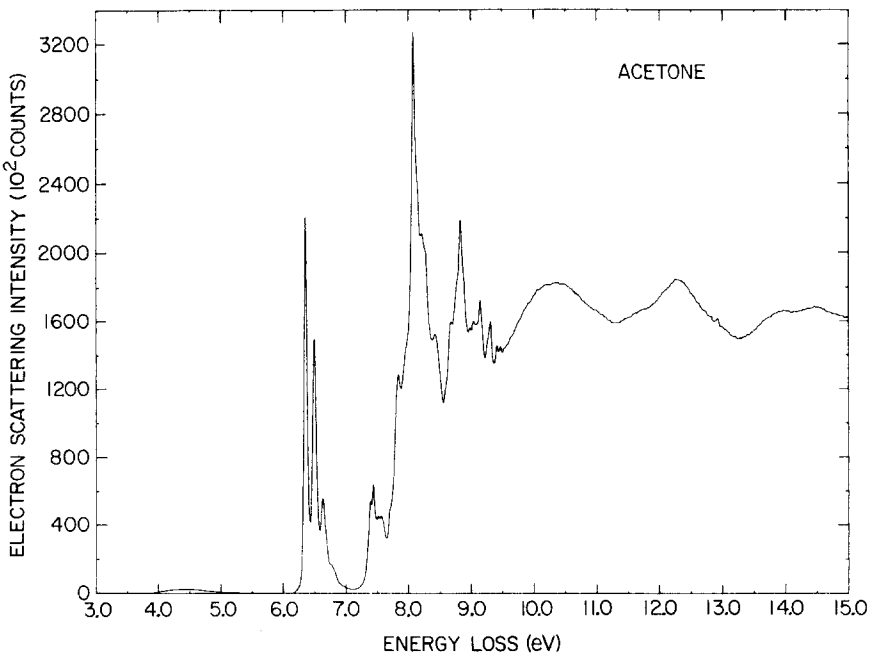

FIG. 3. Energy loss spectrum of acetone from 3 to 15 eV showing the discrete and continuum regions. The weak structure near 12.9 eV is due to trace nitrogen impurity.

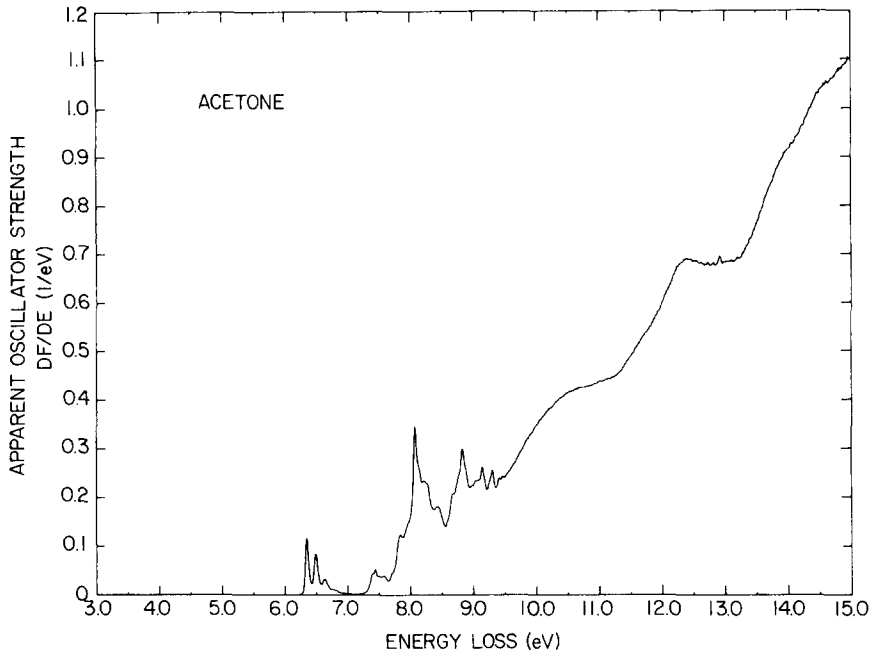

FIG. 4. Apparent oscillator strength distribution of acetone derived from the energy loss data shown in Fig. 3 and normalized to the photoabsorption value at 10.5 eV.

higher order terms in the expansion of $df(K)/dE$ (see Ref. 50) and may limit the accuracy of Eq. (9), particularly when the amount of energy loss represents a substantial fraction of the incident energy (e.g. large E/T). If the absolute energy loss cross section is not determined, then some suitable normalization procedure is needed to fix the relative df/dE values from Eq. (9) on an absolute scale.

To assess the utility of this approach, we have applied Eq. (9) to the electron energy loss spectrum of acetone shown in Fig. 3. The relative oscillator strength values thus derived were normalized to a value of $df/dE = 0.417\ \text{eV}^{-1}$ measured in the continuum region at 10.5 eV by Person and Nicole.[9] The apparent oscillator strength distribution obtained in this manner is presented in Fig. 4.

The spectrum is termed "apparent" in view of several qualifications:

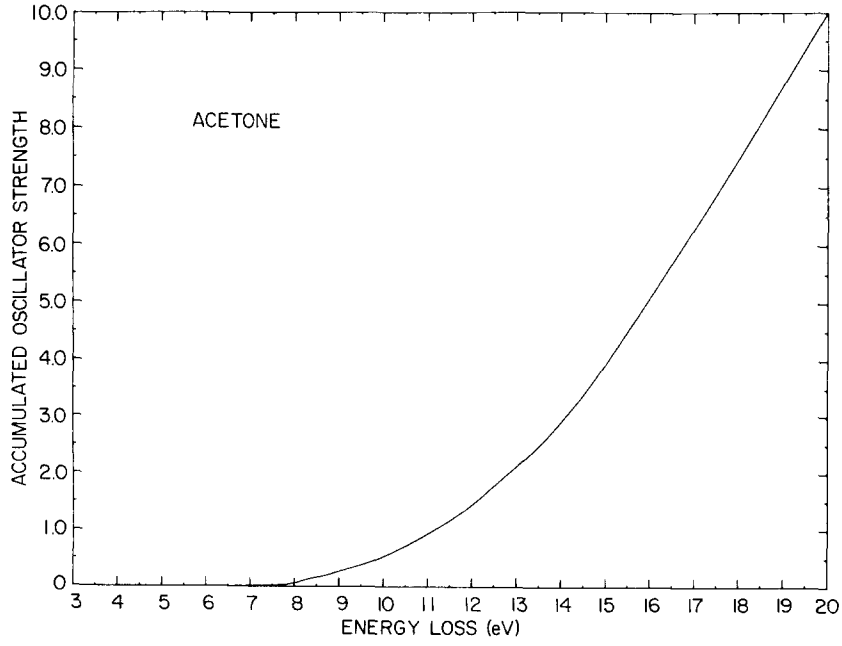

FIG. 5. Accumulated oscillator strength for acetone.

TABLE III. Oscillator strengths[a] for acetone.

Energy (eV)	Oscillator strength values Electron impact	Optical	Reference
3.7–5.9	4.39×10^{-4}	4×10^{-4}	22
6.0–7.1	2.09×10^{-2}	2.0×10^{-2}	6
		2.6×10^{-2}	11
		4.6×10^{-2}	7
9.56	0.253 eV^{-1}	0.249 eV^{-1}	9
9.75	0.294	0.292	9
10.01	0.351	0.353	9
10.25	0.388	0.390	9
10.75	0.427	0.423	9
11.00	0.439	0.429	9
11.25	0.448	0.429	9
11.51	0.493	0.456	9
11.78	0.546	0.510	9

[a]Oscillator strength values listed for the first two energy ranges are integrated values between the limits indicated. The remainder of the values listed for each energy are differential df/dE values.

1. The correction is based on the Born approximation which is considered only marginally valid for electrons with incident energies as low as 100 eV.
2. As mentioned previously, the correction neglects all higher terms in the expansion of $df(K)/dE$ that may be important in certain regions of the spectrum.
3. The correction assumes infinitesimal energy resolution which, in reality, is only finite.
4. The energy loss spectrum may include some distortion due to unspecified instrumental effects.

The seriousness of qualifications (1) and (2) are difficult to assess in the present situation and are in a sense being explored in this study. Although the assumption embodied in point (3) is entirely justified in regions of continuous energy absorption, it is not valid in regions where sharp discrete structures may have a natural energy width smaller than the instrumental resolution. In the latter case, only the integrated oscillator strength, $f=\int (df/dE)\,dE$, is proportional to the integrated peak intensity, and this presents no real difficulty, provided only integrated values are compared for those spectral regions where sharp, discrete structures are observed. Inasmuch as experimental design can minimize instrumental distortion of the spectrum, point (4) is expected to have a small influence on the derived oscillator strength values.

Oscillator strength values derived from the energy loss data are compared with optically measured values in Table III. Agreement to better than ±10% is observed over the entire range (10 to 11.78 eV) of the photoabsorption data of Person and Nicole.[9] Integrated oscillator strengths for the lower lying $\tilde{A}-\tilde{X}\ ^1A_1$ and $\tilde{B}-\tilde{X}\ ^1A_1$ bands also agree very well with various optical measurements. The electron impact data yield integrated oscillator strength values of 0.46 for all transitions below the I.P. at 9.7 eV and of 3.93 for all energy absorption processes below 15 eV. The integrated or accumulated oscillator strength as a function of energy loss for acetone is shown in Fig. 5. To determine the integrated oscillator strength between any two energies, simply subtract the value at the lower energy from that for the higher.

V. SUMMARY

Electron energy loss spectra for acetone vapor have been analyzed in an attempt at unifying available experimental information on the energy absorbing properties of this molecule. Spectroscopic assignments discussed here are in accord with the better established analysis of the formaldehyde spectrum. A comprehensive theoretical effort is needed to assess the degree of interaction between the Rydberg and valence excited states of acetone, which apparently overlap in energy over most of the spectrum. Although the apparent oscillator strengths derived in this work agree well with photoabsorption determinations, only a limited comparison was possible. Additional optical measurements, particularly in the Rydberg region and extending to higher energies in the continuum region, are needed.

ACKNOWLEDGMENTS

We are grateful to Dr. P. Ausloos for discussing his photolysis work with one of us (R. H. H.) and for providing several papers prior to publication. We also thank Dr. M. Inokuti, Dr. J. C. Person, and Dr. M. Krauss for critical readings of this manuscript during its preparation. The help of an ANL undergraduate research trainee, D. L. Lindner, is also acknowledged.

*Work supported in part by the U.S. Atomic Energy Commission.

[1]M. J. Weiss, C. E. Kuyatt, and S. Mielczarek, J. Chem. Phys. **54**, 4141 (1971).
[2]G. C. Pimental and A. L. McClellan, *The Hydrogen Bond* (Freeman, San Francisco, 1970), p. 39.
[3]W. A. Noyes, Jr., A. B. F. Duncan, and W. M. Manning, J. Chem. Phys. **2**, 717 (1934).
[4]A. B. F. Duncan, J. Chem. Phys. **3**, 131 (1935).
[5]M. Lawson and A. B. F. Duncan, J. Chem. Phys. **12**, 329 (1944).
[6]R. S. Holdsworth and A. B. F. Duncan, Chem. Rev. **41**, 311 (1947).
[7]J. S. Lake and A. J. Harrison, J. Chem. Phys. **30**, 361 (1959).
[8]E. E. Barnes and W. T. Simpson, J. Chem. Phys. **39**, 670 (1963).

[9]J. C. Person and P. P. Nicole, Argonne National Laboratory Radiological Physics Division Annual Report, July 1969–June 1970, ANL-7760, Part I, pp. 97–109.
[10]K. J. Watanabe, J. Chem. Phys. **22,** 1564 (1954).
[11]S. L. Lyu, M.S. thesis, University of Hawaii, February 1958.
[12]S. M. Silverman and E. N. Lassettre, J. Chem. Phys. **43,** 194 (1965).
[13]W. T. Naff, R. N. Compton, and C. D. Cooper, J. Chem. Phys. **57,** 1303 (1972).
[14]H. H. Brongersma, Dissertation, University of Leiden, 1968.
[15]C. R. Brundle, M. B. Robin, N. A. Kuebler, and H. Basch, J. Am. Chem. Soc. **94,** 1451 (1972).
[16]M. B. Robin and N. A. Kuebler, J. Mol. Spectrosc. **33,** 274 (1970).
[17]J. A. Simpson, Rev. Sci. Instrum. **35,** 1698 (1964).
[18]C. E. Kuyatt and J. A. Simpson, Rev. Sci. Instrum. **38,** 103 (1967).
[19]J. A. Simpson, *Rec. of the Tenth Symp. on Electron, Ion, and Laser Beam Tech.*, edited by L. Marton (San Francisco Press, San Francisco, 1969), p. 345.
[20]T. Shimanouchi, Natl. Stand. Ref. Data Ser. **17** (1968).
[21]V. I. Vakhlueva, A. G. Finkel, L. M. Sverdlov, and L. A. Zaitseva, Opt. Spektrosk. **25,** 160 (1968).
[22]H. L. McMurry, J. Chem. Phys. **9,** 231 (1941).
[23]C. N. R. Rao, *Ultraviolet and Visible Spectroscopy* (Plenum, New York, 1967), p. 129.
[24]N. L. Allinger, T. W. Stuart, and J. C. Tai, J. Am. Chem. Soc. **90,** 2809 (1968).
[25]K. Yates, S. L. Klemenko, and I. G. Csizmadia, Spectrochim. Acta A **25,** 765 (1969).
[26]S. D. Peyerimhoff, R. J. Buenker, W. E. Kammer, and H. Hsu, Chem. Phys. Lett. **8,** 129 (1971).
[27]J. E. Mentall, E. P. Gentieu, M. Krauss, and D. Neuman, J. Chem. Phys. **55,** 5471 (1971).
[28]G. Herzberg, *Molecular Spectra and Molecular Structure. III. Electronic Spectra and Electronic Structure of Polyatomic Molecules* (Van Nostrand, Princeton, NJ, 1966), pp. 550–1, 658.
[29]J. G. Calvert and J. N. Pitts, Jr., *Photochemistry* (Wiley, New York, 1966).
[30]R. B. Cundall and A. S. Davies, Proc. R. Soc. A **290,** 563 (1966).
[31]H. Shaw and S. Toby, J. Phys. Chem. **72,** 2337 (1968).
[32]H. E. O'Neal and C. W. Larson, J. Phys. Chem. **73,** 1011 (1969).
[33]V. K. Potapov and D. N. Shigorin, Russ. J. Phys. Chem. **40,** 101 (1966).
[34]G. M. White, A. J. Yarwood, and D. P. Santry, Chem. Phys. Lett. **13,** 501 (1972).
[35]D. M. Hayes and K. Morokuma, Chem. Phys. Lett. **12,** 539 (1972).
[36]A. Udvarhazi and M. A. El-Sayed, J. Chem. Phys. **42,** 3335 (1965).
[37]W. C. Johnson, Jr. and W. T. Simpson, J. Chem. Phys. **48,** 2168 (1968).
[38]H. Prugger and F. Dörr, Z. Elektrochem. **64,** 2168 (1968).
[39]P. Potzinger and G. von Bünau, Ber. Bunsenges. Phys. Chem. **72,** 195 (1968).
[40]A. G. Leiga and H. A. Taylor, J. Chem. Phys. **41,** 1247 (1964).
[41]L. J. Lin and P. Ausloos, J. Photochem. **1,** 453 (1972/73).
[42]A. B. F. Duncan, *Rydberg Series in Atoms and Molecules* (Academic, New York, 1971), pp. 83–100.
[43]S. R. LaPaglia, J. Mol. Spectrosc. **10,** 240 (1963).
[44]P. Ausloos and S. G. Lias, Radiat. Res. Rev. **1,** 75 (1968).
[45]J. C. Person (personal communication).
[46]R. E. Rebbert and P. Ausloos, J. Res. Natl. Bur. Stand. (U.S.) A **75,** 481 (1971).
[47]H. Hurzeler, M. G. Inghram, and J. D. Morrison, J. Chem. Phys. **28,** 76 (1958).
[48]E. Murad and M. G. Inghram, J. Chem. Phys. **40,** 3263 (1964).
[49]F. H. Dorman, J. Chem. Phys. **42,** 65 (1965).
[50]M. Inokuti, Rev. Mod. Phys. **43,** 297 (1971).